Block versus Random Amphiphilic Glycopolymer Nanopaticles as Glucose-Responsive Vehicles

ARTICLE *in* BIOMACROMOLECULES · SEPTEMBER 2015

Impact Factor: 5.75 · DOI: 10.1021/acs.biomac.5b01020

8 AUTHORS, INCLUDING:

Qianqian Guo

Nankai University

9 PUBLICATIONS **54** CITATIONS

SEE PROFILE

Xinge Zhang

Nankai University

58 PUBLICATIONS **980** CITATIONS

SEE PROFILE

Chaoxing Li

Nankai University

55 PUBLICATIONS **873** CITATIONS

SEE PROFILE

Article

pubs.acs.org/Biomac

Block versus Random Amphiphilic Glycopolymer Nanopaticles as Glucose-Responsive Vehicles

Qianqian Guo,[†] Tianqi Zhang,[†] Jinxia An,[†] Zhongming Wu,[‡] Yu Zhao,[†] Xiaomei Dai,[†] Xinge Zhang,*[,†] and Chaoxing Li[†]

[†]Key Laboratory of Functional Polymer Materials of Ministry Education, Institute of Polymer Chemistry, Nankai University, Tianjin 300071, China

[‡]2011 Collaborative Innovation Center of Tianjin for Medical Epigenetics, Key Laboratory of Hormones and Development (Ministry of Health), Metabolic Diseases Hospital, Tianjin Medical University, Tianjin 300070, China

Supporting Information

ABSTRACT: To explore the effect of polymer structure on their self-assembled aggregates and their unique characteristics, this study was devoted to developing a series of amphiphilic block and random phenylboronic acid-based glycopolymers by RAFT polymerization. The amphiphilic glycopolymers were successfully self-assembled into spherically shaped nanoparticles with narrow size distribution in aqueous solution. For block and random copolymers with similar monomer compositions, block copolymer nanoparticles exhibited a more regular transmittance change with the increasing glucose level, while a more evident variation of size and quicker decreasing tendency in I/I_0 behavior in different glucose media were observed for random copolymer nanoparticles. Cell viability of all the polymer nanoparticles investigated by MTT assay was higher than 80%, indicating that both block and random copolymers had good cytocompatibility. Insulin could be encapsulated into both nanoparticles, and insulin release rate for random glycopolymer was slightly quicker than that for the block ones. We speculate that different chain conformations between block and random glycopolymers play an important role in self-assembled nanoaggregates and underlying glucose-sensitive behavior.

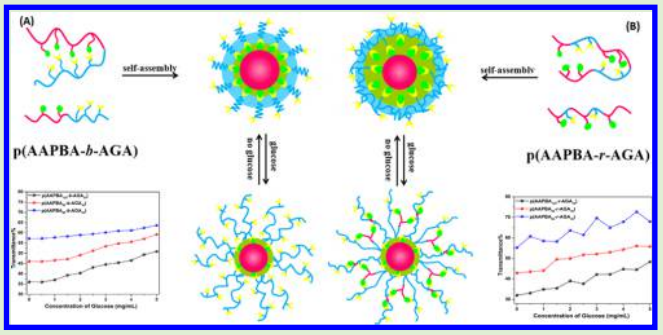

INTRODUCTION

Stimuli-responsive polymer nanoparticles have drawn increasing interests in drug delivery due to their various advantages.[1−5] These polymer nanoparticles could trigger drug release in response to local environmental conditions such as pH,[6] temperature,[7] light,[8] ionic strength,[9] magnetic field[10] and glucose.[11−14] Among these stimuli, a most important one is glucose molecule, because insulin-dependent diabetes mellitus characterized by accumulating glucose concentrations in the blood has been a major global public health epidemic.[12,15] Moreover, the current treatment for diabetes requires persistent monitoring of blood glucose levels and multiple daily insulin injections.[16] This injection not only impinges on the patient quality of life but also fails to precisely control the insulin dosage. An overdose of insulin causes an excessive decrease in blood glucose level, which leads to serious hypoglycemia. Long-acting (basal) insulin analogues have become increasingly popular for the treatment of diabetes mellitus, the main reason is that they can provide clinic advantages over conventional insulin, such as avoidance of hypoglycemia and lower weight gain, ease of insulin device use, and reduction in the number of insulin injections per day. These artificial kinds of insulin, however, do not effectively control blood glucose levels after meals,[17,18] and some of them may speed up the development of cancer.[19,20] Therefore, it would be highly desirable to design and synthesize biocompatible materials for insulin release to match the patients' physiological needs at the proper time and/or the proper sites. The development of glucose-responsive polymers that allow for the construction of a self-regulated insulin delivery system would be significant in the treatment of diabetes. To date, much attention has been spent looking for the proper glucose-responsive systems as insulin carriers to study their potential in the treatment of diabetes. The most attracting glucose-responsive system is phenylboronic acid and its derivatives-based copolymer nanoparticles. The reasons are that (1) phenylboronic acid and its derivatives are versatile enough to be used in different designs and more stable than protein-based systems (glucose oxidase and concanavalin A);[21] (2) polymer nanoparticles are capable of being modified and functionalized by incorporating different functional molecules,[22−24] and can protect the loaded drugs such as protein drugs from damage by the ambient environment.[25−30]

As a result, phenylboronic acid and its derivatives-based polymeric nanoparticles as glucose-responsive systems have

Received: July 29, 2015
Revised: September 21, 2015

DOI: 10.1021/acs.biomac.5b01020
Biomacromolecules XXXX, XXX, XXX−XXX

Table 1. Constitution of Amphiphilic Copolymers

sample		monomer	RAFT agent (mM)	conv (wt %)[a]	AAPBA/AGA (mol/mol) theory[b]	AAPBA/AGA (mol/mol) ^{1}H NMR[c]
p(AAPBA$_{60}$-*b*-AGA$_{30}$)	AGA	-	pAAPBA$_{60}$	80.29	2	1.54
p(AAPBA$_{90}$-*b*-AGA$_{30}$)	AGA	-	pAAPBA$_{90}$	76.19	3	3.17
p(AAPBA$_{120}$-*b*-AGA$_{30}$)	AGA	-	pAAPBA$_{120}$	84.33	4	3.96
p(AAPBA$_{60}$-*r*-AGA$_{30}$)	AGA	AAPBA	DMP	81.92	2	1.46
p(AAPBA$_{90}$-*r*-AGA$_{30}$)	AGA	AAPBA	DMP	88.44	3	3.05
p(AAPBA$_{120}$-*r*-AGA$_{30}$)	AGA	AAPBA	DMP	76.88	4	3.78

[a]Calculated via weight method. [b]The theoretical weight ratio of AAPBA/AGA. [c]The approximate block and random copolymer compositions were calculated using the ^{1}H NMR integral intensity of the signal between the 4H in phenyl moiety (6.8−7.8 ppm) and 5H in sugar moiety.

been actively investigated.[28−39] Among these glucose-responsive systems, block copolymer has drawn much more attention for their regular structures and easily self-assembling to core−shell nanoparticles.[31−39] Jin et al. synthesized a thermoresponsive poly(ethylene oxide)-*b*-poly(methoxydi(ethylene glycol) methacrylate-*co*-aminophenylboronic acid ethyl methacrylate) where phenylboronic acid acted as the sugar- and pH-responsive trigger to tune the multiple micellization.[31] Jennifer et al. developed poly(3-acrylamidophenylboronic acid pinacol ester)-*b*-poly(*N*,*N*-dimethylacrylamide) and studied the sugar- and pH-responsive behaviors.[34] Previously, our group has established phenylboronic acid-based block glycopolymer and explored their potential as glucose-responsive vehicles in drug delivery.[36−38] Although block polymers play an important role in these copolymers, it should be noted that random copolymer with the similar polymeric configuration exhibited good stimuli-response behaviors.[40−44] Tian et al. prepared amphiphilic random copolymer that showed photoresponse behavior.[40] Chi et al. displayed a novel thermo- and photoresponsive polypseudorotaxane between pillararene WP7 and an azobenzene-containing random copolymer.[41] Moreover, our group has successfully prepared random glycopolymer nanoparticles with good glucose-responsive behaviors.[43,44] It has been identified that copolymer with block or random structure usually generated different effects on their properties.[45−50] Oda et al. explored the effect of block and random amphiphilic copolymers with similar monomer compositions on antibacterial activities.[48] Shao et al. synthesized a series of block and random thermosensitive copolymers consisting of oligo(ethylene glycol) and cholic acid pendant groups, and found that block copolymer nanoparticles exhibited a different thermosensitive behavior in the same temperature range compared with the random ones.[49]

To explore the effect of amphiphilic copolymer structures on their glucose-responsive behaviors, we developed amphiphilic phenylboronic acid-based glycopolymers with block and random sequences by RAFT polymerization. By qualifying the feed molar ratio of two monomers of 3-acryl aminophenylboronic acid (AAPBA) and 2-(acrylamido) glucopyranose (AGA) to chain transfer agent, a series of amphiphilic block and random glycopolymers were obtained. The formation mechanism and glucose-sensitive behaviors of two kinds of polymer aggregates were investigated, and in vitro release of insulin in response to different glucose media was further evaluated.

EXPERIMENTAL SECTION

Materials. 3-Aminophenylboronic acid monohydrate was purchased from Nanjing Kangmanlin Chemical Industry Co. Ltd. (Nanjing, China). Acryloyl chloride was prepared by refluxing acrylic acid and thionyl chloride at 75 °C for 8 h and freshly distilled before used. 2-Dodecylsulfanylthiocarbonylsulfanyl-2-methylpropionic acid (DMP) was synthesized according to the method as previously reported.[51,52] D-Glucosamine hydrochloride was supplied by Beijing Ouhe Technology Co. Ltd. (Beijing, China). 2,2′-Azobis(isobutyronitrile) (AIBN) was recrystallized twice from ethanol and dried in vacuum before used. Pure crystalline porcine insulin was purchased from Xuzhou Wangbang Biochemical Co. Ltd. (Xuzhou, China). 3-[4,5-Dime-thylthiazol-2-yl]-2,5-diphenyltetrazolium bromide (MTT) was obtained from Beyotime Institute of Biotechnology (Nantong, China). Other reagents were of analytical grade and used as received.

Synthesis of 2-(Acrylamido) Glucopyranose (AGA). AGA was synthesized by the previously reported method.[53] Briefly, D-glucosamine hydrochloride (10.0 g, 4.64×10^{-2} mol) and potassium carbonate (6.41 g, 4.64×10^{-2} mol) were dissolved in methanol (250 mL) in a 500 mL single neck round-bottom flask. The flask was cooled to −10 °C using an acetone/ice bath before acryloyl chloride (3.77 g, 4.17×10^{-2} mol) was added dropwise into the mixture under vigorous stirring. The mixture was stirred in ice bath for 30 min and then reacted for another 3 h at room temperature. The crude mixture was concentrated under reduced pressure to off-white slurry. The slurry was purified via silica gel column chromatography using dichloromethane/methanol (v/v, 4:1) as eluent. The white solid exited the column with the R_f value of 0.33, with 58% conversion obtained gravimetrically.

Synthesis of Poly(3-acrylamidophenylboronic acid) (pAAPBA). The monomer of AAPBA was prepared using the modified method described by Lee et al.[54] Briefly, 3-aminophenylboronic acid monohydrate (5.0 g, 3.22×10^{-2} mol) was dissolved in sodium hydroxide solution (40 mL, 0.129 mol) and cooled in an ice bath. Freshly distilled acryloyl chloride (3.2 mL, 4.0×10^{-2} mol) was added dropwise to 3-aminophenylboronic acid monohydrate solution over 1 h. The reaction mixture was stirred for further 2 h at room temperature and adjusted to pH 8 using 0.1 M HCl. The resulting precipitation was filtered and washed with cold water. The precipitate was dissolved in distilled water after heating to 80 °C, and the insoluble residues were filtered off. The filtrate was left to stand overnight at 4 °C, and the resulting crystals were filtered, and dried under a vacuum.

pAAPBA was synthesized by RAFT polymerization, using DMP as RAFT agent, AIBN as initiator by the previously reported method.[55] Briefly, AAPBA and a certain amounts of DMP and AIBN were dissolved in *N*,*N*-dimethylformamide (DMF); then the mixture was purged with nitrogen for 30 min and transferred to a water bath preheated to 70 °C. The reaction was quenched after 10 h by cooling in an ice bath for 5 min. The resultant polymer was isolated by precipitating with acetic ether three times, and drying under vacuum. By changing feed molar ratio of AAPBA to DMP (120:1, 90:1, and 60:1), three different homopolymers were obtained, marked as pAAPBA$_{120}$, pAAPBA$_{90}$, and pAAPBA$_{60}$, respectively.

Synthesis of Block and Random Phenylboronic Acid-Based Glycopolymers. RAFT copolymerization was performed at [AGA]/

DOI: 10.1021/acs.biomac.5b01020
Biomacromolecules XXXX, XXX, XXX−XXX

Scheme 1. Synthesis of (A) Block Copolymer p(AAPBA-*b*-AGA) and (B) Random Copolymer p(AAPBA-*r*-AGA)

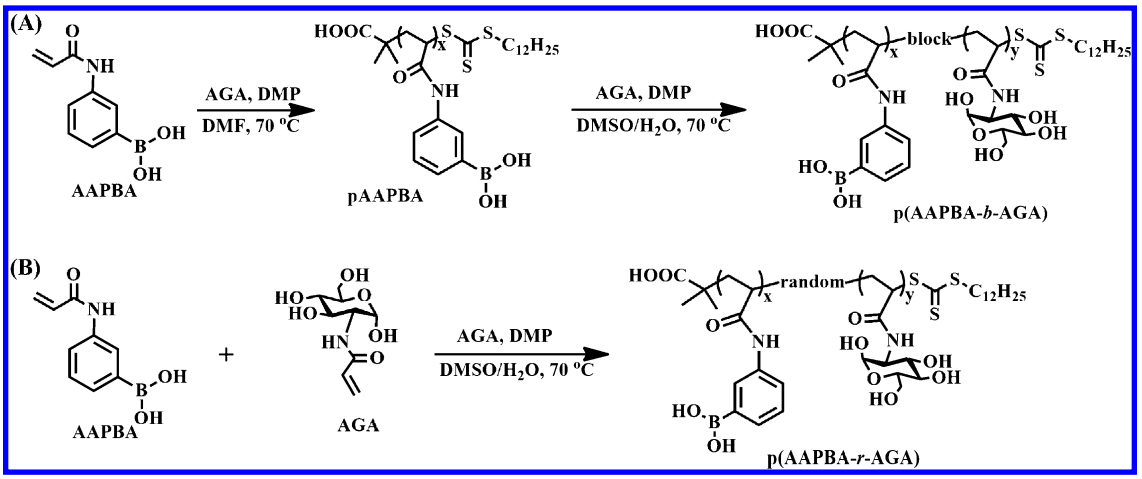

[RAFT agent]/[AIBN] = 30:1:1 using AGA as monomer, homopolymer pAAPBA as macroRAFT agent, AIBN as initiator, and DMF/water (v/v, 19:1) as mixed solvents. The reaction system was placed in a preheated oil bath at 70 °C for 12 h following nitrogen purging for 30 min. The polymerization was quenched by cooling in an ice bath for 5 min. The resultant polymer was obtained by precipitating with acetic ether three times, and drying under vacuum. By changing the ratio of pAAPBA macroRAFT to the AGA, we obtained three distinct block copolymers and these were named as p(AAPBA$_{120}$-*b*-AGA$_{30}$), p(AAPBA$_{90}$-*b*-AGA$_{30}$), and p(AAPBA$_{60}$-*b*-AGA$_{30}$) (Table 1).

Random copolymer p(AAPBA-*r*-AGA) was synthesized by RAFT polymerization using AAPBA and AGA as two monomers, DMP as RAFT agent, AIBN as initiator, and DMF/water (v/v, 19:1) as mixed solvents. The copolymerization was performed at [AAPBA]/[AGA]/[DMP]:[AIBN] = 120:30:1:0.5. After the solution was purged with N_2 for 30 min, the reaction system was allowed to stir at 70 °C for 12 h, and then polymerization was quenched by cooling in an ice bath for 5 min. The resultant copolymer was precipitated, filtered, washed with acetic ether and subsequently dried under a vacuum. By changing the molar ratio of AAPBA and AGA to DMP, we obtained and named three distinct random copolymers as p(AAPBA$_{120}$-*r*-AGA$_{30}$), p-(AAPBA$_{90}$-*r*-AGA$_{30}$), and p(AAPBA$_{60}$-*r*-AGA$_{30}$), respectively (Table 1).

Characterization of Glycopolymers. ^{1}H NMR spectra were recorded at room temperature using a Varian Unity-plus 400 NMR spectrometer. FT-IR spectra was recorded on a Fourier Transform Infrared Spectrometer (FTS-6000, Bio-Rad Co.) using a KBr tablet containing the sample powder at a resolution of 8 cm^{-1}. The thermogravimetric analysis of copolymer, using 10 mg sample, was conducted in nitrogen using a thermogravimetric analyzer (TGA, STA409PC) at a heating rate of 10 °C/min.

Preparation Copolymer Nanoparticles. Copolymer nanoparticles were prepared according to the previously reported method.[56] Briefly, 10 mg of polymer was dissolved in 2 mL of mixed solvents containing DMSO and water (v:v, 1:1), and then 20 mL of water was slowly added to the solution under vigorous stirring. After 12 h, the solution was transferred to a dialysis tube (MWCO 3500) and dialyzed against water for 24 h. The organic solvent was removed by replacing water every 3 h, and then the nanoparticle solution was centrifuged at 12 000 rpm for 20 min. Finally, blank nanoparticles were obtained after freeze-drying the suspension.

Insulin-loaded nanoparticles were prepared in a similar method. Five milligrams of insulin was dissolved in 20 mL of water and this mixture was slowly added to the copolymer solution under stirring. After 12 h, the solution was transferred to a dialysis tube (MWCO 3500). After dialysis for 24 h, insulin-loaded nanoparticles suspension was centrifuged at 12 000 rpm for 20 min. Finally, the precipitate was washed with deionized water and centrifuged three times prior to lyophilization. The amount of free insulin in the supernatant was monitored by Bradford method using a UV spectrometer (Shimadzu UV-2550) at 595 nm.[57] Insulin encapsulation efficiency (EE) and loading capacity (LC) were calculated using the following equations:

$$\text{EE\%} = \frac{\text{total insulin} - \text{free insulin}}{\text{total insulin}} \times 100$$

$$\text{LC\%} = \frac{\text{total insulin} - \text{free insulin}}{\text{NPs weight}} \times 100$$

Characterization of Nanoparticles. ^{11}B NMR spectra of copolymer nanoparticles were recorded at room temperature using a Varian Unity-plus 400 NMR spectrometer. The ^{11}B chemical shifts were measured at relative external boron trifluoride diethyl etherate ($BF_3{\cdot}O(C_2H_5)_2$) setting as 0 ppm. Hydrodynamic diameter (D_H) and size distribution of nanoparticles were characterized by dynamic light scattering (DLS) using a Malvern Zetasizer Nano S apparatus equipped with a 4.0 mV laser operating at λ = 636 nm. All measurements were performed at a scatting angle of 90°. The morphological characteristics of nanoparticles were observed using transmission electron microscope (TEM, Philips EM400ST). Samples were placed on copper grids coated with Formvar films for observation under TEM. The turbidity measurement was conducted using a UV spectrometer (Shimaszu, UV-2550) at 500 nm.

Cell Viability. Cell viability of block and random copolymers was evaluated by using NIH3T3 cells. The cell lines were cultured in Dulbecco's modified Eagle's medium (DMEM, Gibco) supplemented with 10% fetal bovine serum, 1% penicillin/streptomycin and 1% nonessential amino acid in 5% CO_2/95% air at 37 °C. Cells were seeded in a 96-well plate at a density of 10^4 cells per well. The polymer nanoparticles were diluted with culture medium to achieve the predetermined concentrations. The medium in the wells was replaced with the preprepared sample solution. After 24 h of incubation, 10 μL of MTT solution was added into each well and the mixture was incubated for further 4 h. The medium was removed and 150 μL of DMSO was added to each well to dissolve the formazane crystals. The optical density was read on a microplate reader at 492 nm in triplicate. Relative cell viability was calculated as a percentage compared with that of untreated control.

In Vitro Drug Release. In vitro insulin release from different nanoparticles was investigated by incubating 6 mg of insulin-loaded nanoparticles in 2 mL of pH 7.4 phosphate buffer solution (PBS, 0.1 M) containing different glucose concentrations at 37 ± 0.5 °C with shaking (100 rev/min). At a predetermined time, samples were centrifuged at 12 000 rpm for 5 min, and 100 μL of supernatant was withdrawn and replaced with the same volume of fresh medium. The amount of insulin was monitored using Bradford method. Each sample was analyzed in triplicate and results were reported as mean ± standard deviation (n = 3).

DOI: 10.1021/acs.biomac.5b01020
Biomacromolecules XXXX, XXX, XXX−XXX

To determine the insulin release mechanism, release data were analyzed using the Ritger-Peppas equations.[58]

$$M_t/M^{\infty} = kt^n$$

where M_t and M_∞ are the absolute cumulative amount of drug released to time t and infinite time, respectively, and k is a structural/geometric constant. n is related to the Fickian diffuse mechanism, non-Fickian diffuse mechanism, and bulk erosion mechanism of release as values of $n < 0.43$, $0.43 < n < 0.85$, and $n > 0.85$, respectively.

RESULTS AND DISCUSSION

Synthesis and Characterization of Block and Random Copolymers. Fabrications of block copolymer p(AAPBA-*b*-AGA) and random copolymer p(AAPBA-*r*-AGA) were carried out by RAFT polymerization as shown in Scheme 1. A series of copolymers were obtained by changing the molar ratio of monomers to the corresponding RAFT agent. To confirm the structure difference, ^{1}H NMR spectra of AAPBA, pAAPBA and p(AAPBA-*b*-AGA) were analyzed (Figure S1). In the spectrum of AAPBA, peaks at 5.7, 6.3, and 6.5 ppm were assigned to protons on double bond, and signals at 7.3−8.0 ppm were assigned to protons on benzene ring. Compared with the spectrum of AAPBA, signals of double bond in pAAPBA completely disappeared, and peaks of phenyl group at 6.8−7.8 ppm were retained, confirming the successful preparation of pAAPBA. After copolymerization of pAAPBA and AGA, the new resonance signals in p(AAPBA$_{120}$-*b*-AGA$_{30}$) appeared in the ranges of 0.8−2.2 and 3.0−3.8 ppm, which were assigned to protons from main chain and sugar residue, respectively, indicating p(AAPBA-*b*-AGA) copolymer was synthesized successfully. ^{1}H NMR spectra of AAPBA, AGA and p(AAPBA$_{120}$-*r*-AGA$_{30}$) were further analyzed. As shown in Figure S2, signals at 3.4−4.0 ppm were ascribed to protons on the sugar residue in AGA, and peaks at 5.2, 5.8, and 6.3 ppm assigned to protons on double bond. Compared with the spectra of AGA and AAPBA, it is obvious that signals of double bond disappeared and protons on the newly formed main chain generated signals at 0.8−2.4 ppm in the spectrum of p(AAPBA$_{120}$-*r*-AGA$_{30}$). Both typical signals of phenyl (6.8−8.0 ppm) and sugar residue (2.8−3.8 ppm) were preserved in the spectrum of random copolymer. These results imply that block and random copolymers were successfully prepared. The AAPBA/AGA composition in block and random copolymers was calculated using ^{1}H NMR integral intensity of signals between the 4H in phenyl moiety and 5H in sugar moietiesy (Table 1). Compared with the composition of block and random copolymers, block copolymer contained more AAPBA content than the corresponding random one, which was due to the lower reactive activity of pAAPBA as macroRAFT than that of DMP.

Compared with the spectra of p(AAPBA$_{120}$-*b*-AGA$_{30}$) and p(AAPBA$_{120}$-*r*-AGA$_{30}$) in Figure 1, we found that the features of peaks from sugar residue and phenyl group in block and random copolymers were different. Peaks of sugar residue for block copolymer showed a slightly serrated shape while the peak shape was like a mountain for random one. And the peak shape of phenyl group between block and random copolymers was slightly different. The results were attributed to the different distribution of sugar and phenylboronic acid moiety in the copolymers.

Figure 2 showed FT-IR spectra of pAAPBA$_{120}$, p(AAPBA$_{120}$-*b*-AGA$_{30}$) and p(AAPBA$_{120}$-*r*-AGA$_{30}$). In the spectrum of pAAPBA$_{120}$, peak absorption band of 3313 cm^{-1} was due to

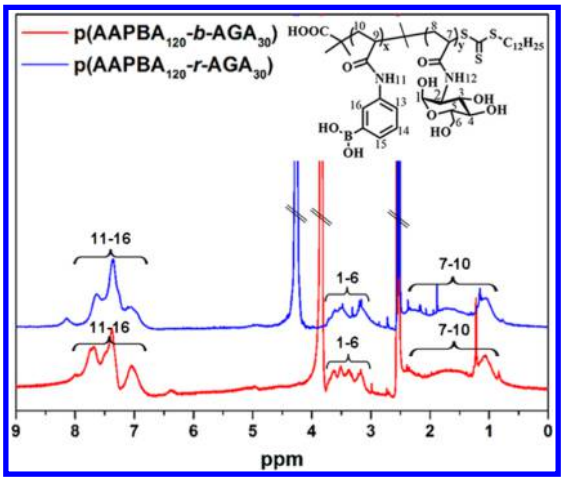

Figure 1. ^{1}H NMR spectra of p(AAPBA$_{120}$-*b*-AGA$_{30}$) and p(AAPBA$_{120}$-*r*-AGA$_{30}$) (the mixed solvents of DMSO-d_6/D$_2$O, v/v = 19:1).

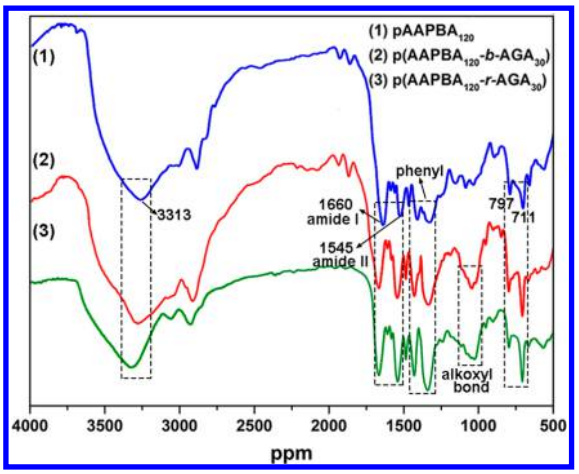

Figure 2. FT-IR spectra of pAAPBA$_{120}$, p(AAPBA$_{120}$-*b*-AGA$_{30}$), and p(AAPBA$_{120}$-*r*-AGA$_{30}$).

N−H stretching. Amide I band was assigned to C═O stretching resulted in an absorption band of 1660 cm^{-1}, while an absorption band at 1545 cm^{-1} was attributed to N−H bending vibration (amide II band) of a secondary amide. In addition, the typical absorption bands of phenyl ring in pAAPBA$_{120}$ from 1500 to 1300 cm^{-1} region and absorption peaks at 797 and 711 cm^{-1} were observed. In comparison with pAAPBA$_{120}$, p(AAPBA$_{120}$-*b*-AGA$_{30}$) maintained the typical absorption of pAAPBA$_{120}$ described above. And band in 1200−1000 cm^{-1} region resulted from C−O stretching corresponding to alkoxyl bond in carbohydrate moiety. The FT-IR spectrum of p(AAPBA$_{120}$-*r*-AGA$_{30}$) was similar to that of p(AAPBA$_{120}$-*b*-AGA$_{30}$) indicating that block and random copolymers were successfully synthesized.

To evaluate the effect of copolymer structure on their thermostability, thermogravimetric analysis was performed. Thermogravimetric (TG) and derivative thermogravimetric (DTG) curves for p(AAPBA$_{120}$-*b*-AGA$_{30}$) and p(AAPBA$_{120}$-*r*-AGA$_{30}$) were shown in Figure 3. Compared with TG and DTG curves of two copolymers, there was profoundly different degradation phenomenon. It can be seen from DTG curves that there were three distinct degradations at about 63, 134, and 308 °C for p(AAPBA$_{120}$-*b*-AGA$_{30}$), and 63, 230, and 382 °C for

DOI: 10.1021/acs.biomac.5b01020
Biomacromolecules XXXX, XXX, XXX−XXX

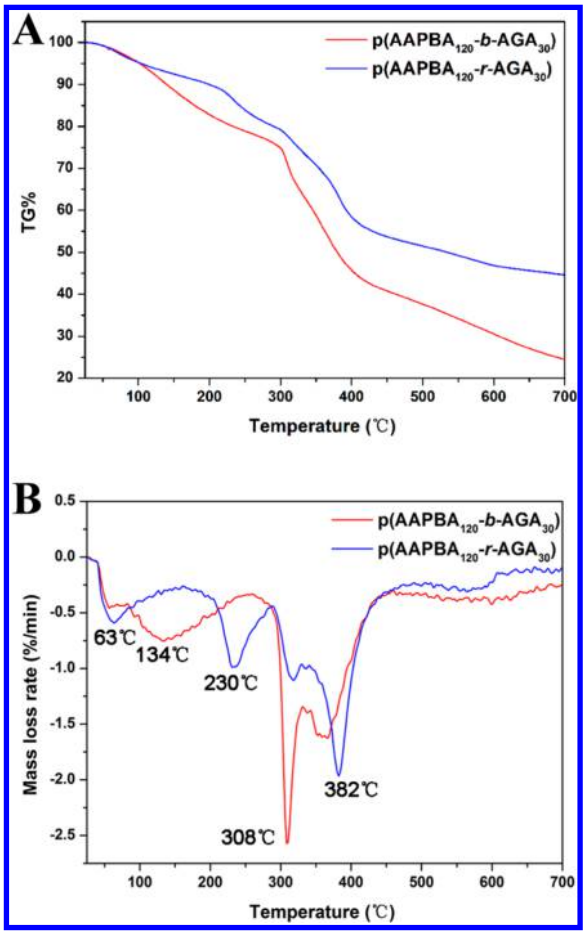

Figure 3. Thermal analysis of copolymers. TG (A) and DTG (B) curves for p(AAPBA$_{120}$-*b*-AGA$_{30}$) (red) and p(AAPBA$_{120}$-*r*-AGA$_{30}$) (blue).

p(AAPBA$_{120}$-*r*-AGA$_{30}$), respectively. For two copolymers, the first degradation at 63 °C was assigned to free water and to water linked by hydrogen bonds. The second degradation, which was maximized around 130 °C for p(AAPBA$_{120}$-*b*-AGA$_{30}$) while for p(AAPBA$_{120}$-*r*-AGA$_{30}$) it took place at 230 °C, corresponded to the thermal decomposition of the pendent sugar residues. We deduce that the higher temperature in the second degradation for random copolymer was attributed to more boronate complex between phenylboronic acid and sugars with the consequent improvement in thermal stability of pendent sugar residues. The last stage of thermal degradation was assigned to the thermal degradation of the backbone. At this stage, the 30% of weight loss temperature for p(AAPBA$_{120}$-*b*-AGA$_{30}$) was 308 °C, whereas that of p(AAPBA$_{120}$-*r*-AGA$_{30}$) was 382 °C with 43% of weight loss. These results were in accordance with the previous reports.[37,44] The above results show that the copolymer structure plays an important role in their thermal decomposition.

Preparation and Characterization of Copolymer Nanoparticles. In current work, the synthesized amphiphilic copolymers were self-assembled to nanoparticles using the nanoprecipitation method. In addition to the intrinsic amphiphilicity, the complexation of AAPBA with the glucosamine moietiy in AGA also promoted the copolymer self-assembled process (Scheme 2). This is because a glucose molecule can complex with two boronic acids at its 4-OH, 5-CH_2OH of glucosamine, leading to inter- or intramolecular interaction.[59,60] The morphology and size of nanoparticles were observed using TEM and DLS. As shown in Figure 4, TEM analysis demonstrates that nanoparticles were spherical in shape with good dispersion. The D_H determined by DLS for blank p(AAPBA-*b*-AGA) and p(AAPBA-*r*-AGA) nanoparticles was in the range of 83−130 and 91−140 nm, with the polydispersity index (PDI) between 0.066 and 0.174, respectively (Table 2). For the copolymers with similar monomer composition, the average D_H for p(AAPBA-*r*-AGA) nanoparticles was larger than that of the corresponding p(AAPBA-*b*-AGA), most probably due to more boronic ester linkages in p(AAPBA-*r*-AGA) nanoparticles enhancing the swelling of nanoparticles.

To confirm whether there was more boronate complex between phenylboronic acid and sugars, we measured the relative content of free boronic and boronate complex in p(AAPBA$_{120}$-*b*-AGA$_{30}$) and p(AAPBA$_{120}$-*r*-AGA$_{30}$) nanoparticles using ^{11}B NMR spectra. As shown in Figure 5, the spectra

Scheme 2. Self-Assembly of (A) Block and (B) Random Copolymers into Nanoparticles in Aqueous Solution without/with Glucose

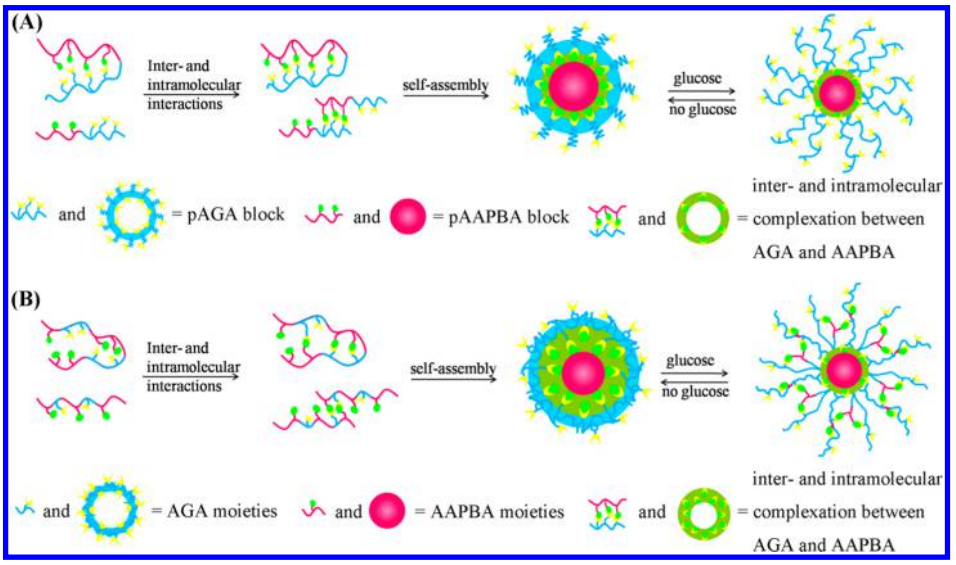

DOI: 10.1021/acs.biomac.5b01020
Biomacromolecules XXXX, XXX, XXX−XXX

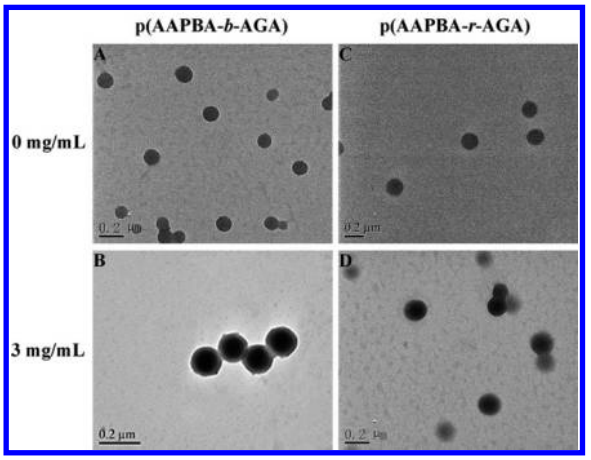

Figure 4. TEM photographs of copolymer nanoparticles before and after treatment with 3 mg/mL of glucose medium: (A and C) p(AAPBA-*b*-AGA) nanoparticles; (B and D) p(AAPBA-*r*-AGA) nanoparticles.

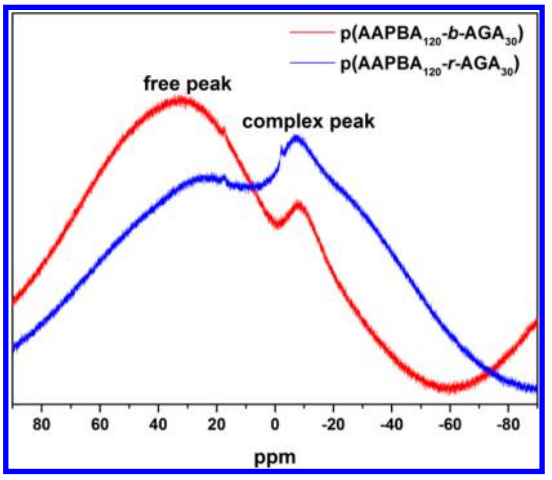

Figure 5. ^{11}B NMR spectra of p(AAPBA$_{120}$-*b*-AGA$_{30}$) and p(AAPBA$_{120}$-*r*-AGA$_{30}$) nanoparticles (D_2O).

consist of two peaks: free boronic peak and boronate complexed peak for both nanoparticles.[61,62] The boronate complexed peak intensity was higher than the free boronic acid peak intensity in the spectrum of p(AAPBA$_{120}$-*r*-AGA$_{30}$) nanoparticles, while there was an inverse result for p(AAPBA$_{120}$-*b*-AGA$_{30}$) nanoparticles. This indicated that there were more boronate complex being formed during the self-assembled process for p(AAPBA$_{120}$-*r*-AGA$_{30}$) nanoparticles than that for p(AAPBA$_{120}$-*b*-AGA$_{30}$) nanoparticles, which is ascribed to the randomly distribution of phenylboronic acid and sugars in p(AAPBA$_{120}$-*r*-AGA$_{30}$), providing more chance to form boronate complex.

Glucose Sensitivity of Glycopolymer Nanoparticles. Phenylboronic acid and its derivatives are kinds of weak acids with a pK_a of 8.2−8.6, and many efforts have been made to decrease the pK_a to realize the glucose-sensitivity of phenylboronic acid and its derivatives at physiological pH.[21,43,44,63−65] Specially, it has been verified by our group that the glucose-sensitivity of phenylboronic acid at physiological pH was achieved in the presence of sugars.[36,37,44,65] Therefore, introduction of AAPBA moiety could contribute the glucose sensitivity to resultant nanoparticles. Table 3 listed D_H values and PDI of both block and random nanoparticles in pH 7.4 PBS in 1 or 3 mg/mL glucose medium concentrations at 37 °C. After the treatment with glucose, both nanoparticles swelled to larger size than the corresponding blank nanoparticles with PDI ranging from 0.079 to 0.177. The results were in accordance with the phenomenon observed by TEM (Figure 4). It was found in Table 3 that nanoparticles swelled gradually as glucose concentration increased from 0 to 3 mg/mL, which was correlated to glucose-sensitivity of AAPBA moieties in glycopolymer. Moreover, glucose-responsiveness of nanoparticles increased as the content of AAPBA in both block and random glycopolymer increased gradually. These results further confirm that the glucose-sensitivity of AAPBA at physiological pH was achieved due to the presence of AGA.

Due to introduction of phenylboronic acid into block and random copolymers, it is necessary to study the influence of copolymer structure on glucose-sensitivity. Figure 7 shows that the stimulus-responsive behaviors of two copolymer nanoparticles were different in different glucose media. For block polymer nanoparticles, transmittance (%T) showed a tendency to rise with the increment of glucose concentrations, while %T of random copolymer nanoparticles displayed fluctuated movement after the treatment with the same glucose media. The results were ascribed to the different structures of block and random copolymer nanoparticles. Compared with random copolymer nanoparticles, there was clearer and neater self-assembled structure for block ones leading to more regular sugar-sensitive change in different glucose media.

Light scattering intensity (I) of nanoparticles in glucose medium over time was measured by DLS, and I_0 was set as the control value of nanoparticles without the treatment with glucose. I/I_0 values reflected the swelling degree of nanoparticles after the incubation with different glucose media. As shown in Figure 8, I/I_0 values decreased gradually as glucose concentration increased from 0 to 3 mg/mL, which was in agreement with an increase in D_H for all samples. Note that the decrease of I/I_0 values was greater in 3 mg/mL glucose medium than in 1 mg/mL medium for each nanoparticle, which was due to more dissociation of nanoparticles under higher glucose

Table 2. D_H, PDI, and Zeta Potential of Copolymer Nanoparticles[a]

sample	D_H (nm)	PDI	zeta potential (mV)	EE (%)	LC (%)
p(AAPBA$_{60}$-*b*-AGA$_{30}$)	83.1 ± 0.5	0.09 ± 0.01	−21.2 ± 1.3	64.9 ± 3.6	9.7 ± 3.7
p(AAPBA$_{90}$-*b*-AGA$_{30}$)	107.1 ± 3.5	0.17 ± 0.01	−26.6 ± 0.9	57.6 ± 1.7	10.9 ± 2.7
p(AAPBA$_{120}$-*b*-AGA$_{30}$)	129.6 ± 4.0	0.10 ± 0.02	−40.6 ± 0.4	55.6 ± 2.1	12.9 ± 1.4
p(AAPBA$_{60}$-*r*-AGA$_{30}$)	91.0 ± 0.5	0.10 ± 0.01	−15.2 ± 0.7	61.9 ± 1.9	7.5 ± 3.1
p(AAPBA$_{90}$-*r*-AGA$_{30}$)	118.6 ± 4.1	0.11 ± 0.03	−26.2 ± 0.9	52.2 ± 1.1	8.5 ± 0.9
p(AAPBA$_{120}$-*r*-AGA$_{30}$)	140.0 ± 0.6	0.10 ± 0.02	−30.7 ± 0.9	50.1 ± 2.9	10.4 ± 1.1

[a]Each experiment was performed in triplicate and the results were reported as mean ± SD.

DOI: 10.1021/acs.biomac.5b01020
Biomacromolecules XXXX, XXX, XXX−XXX

Table 3. D_H and PDI of Copolymer Nanoparticles in Various Glucose Media Measured by DLS[a]

	glucose concentration (mg/mL)			
	1		3	
samples	D_H (nm)	PDI	D_H (nm)	PDI
p(AAPBA$_{60}$-*b*-AGA$_{30}$)	91.1 ± 0.5	0.09 ± 0.01	95.5 ± 1.7	0.08 ± 0.03
p(AAPBA$_{90}$-*b*-AGA$_{30}$)	109.6 ± 2.7	0.10 ± 0.03	125.2 ± 5.8	0.18 ± 0.01
p(AAPBA$_{120}$-*b*-AGA$_{30}$)	133.8 ± 1.1	0.10 ± 0.03	155.0 ± 2.6	0.12 ± 0.04
p(AAPBA$_{60}$-*r*-AGA$_{30}$)	93.7 ± 1.2	0.11 ± 0.01	115.8 ± 3.2	0.14 ± 0.02
p(AAPBA$_{90}$-*r*-AGA$_{30}$)	126.1 ± 2.8	0.14 ± 0.03	156.7 ± 2.0	0.12 ± 0.02
p(AAPBA$_{120}$-*r*-AGA$_{30}$)	143.2 ± 1.7	0.11 ± 0.01	170.2 ± 2.9	0.11 ± 0.01

[a]Each experiment was performed in triplicate and the results were reported as mean ± SD.

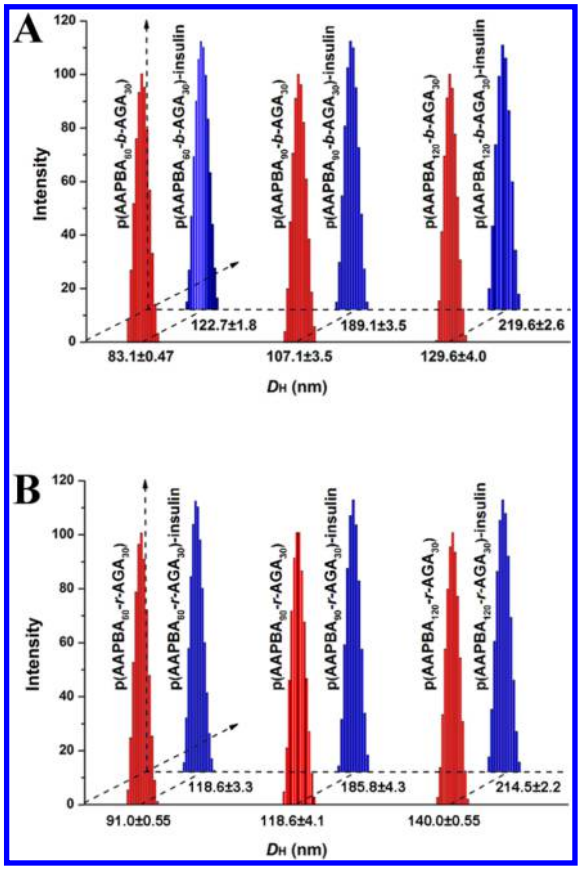

Figure 6. Size and size distribution of empty glycopolymeric nanoparticles and insulin-loaded nanoparticles in pH 7.4 PBS.

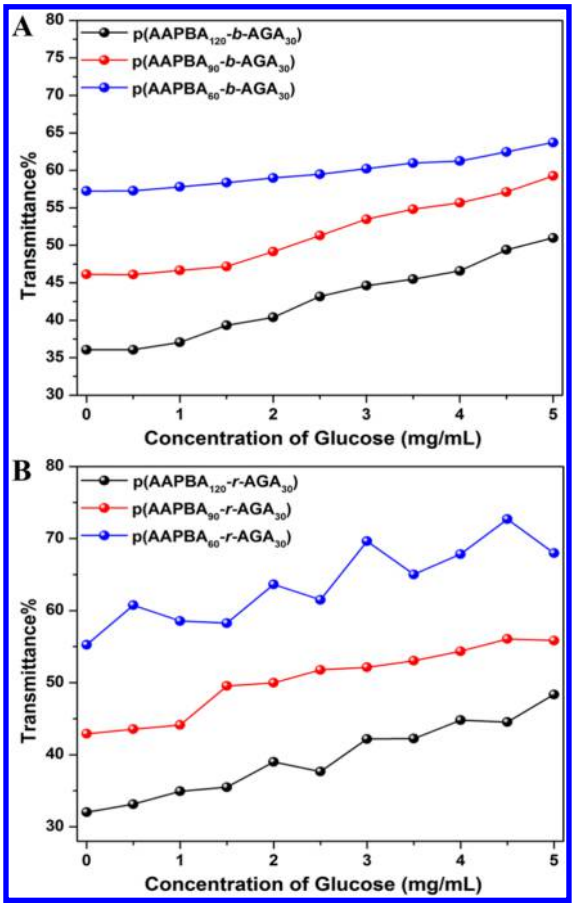

Figure 7. Effect of glucose concentrations on the percent transmittance (%T) of the block copolymer nanoparticles (A) and the random copolymer nanoparticles (B) at pH 7.4.

concentration. And the enhancement of D_H with an increase of glucose concentration significantly illustrated the glucose-sensitivity of nanoparticles. This was attributed to glucose forming a boronate complex with boronic acid derivatives, which was dynamic-covalent, and boronate complex allowing the linkage to reconfigure their structure in the presence of other diols that competed for bonding with the boronic acid. The result was in accordance with that reported by the Sumerlin group.[66,34] Thus, the boronate complex could be induced to dissociate via competitive exchange reactions. Compared with the I/I_0 variation of p(AAPBA-*b*-AGA) and p(AAPBA-*r*-AGA) nanoparticles in 3 mg/mL of glucose solution, I/I_0 final values were 0.73, 0.79, and 0.85 for p(AAPBA$_{60}$-*b*-AGA$_{30}$), p(AAPBA$_{90}$-*b*-AGA$_{30}$), and p(AAPBA$_{120}$-*b*-AGA$_{30}$), respectively, 0.62, 0.72, and 0.76 for p(AAPBA$_{60}$-*r*-AGA$_{30}$), p(AAPBA$_{90}$-*r*-AGA$_{30}$), and p(AAPBA$_{120}$-*r*-AGA$_{30}$), respectively. The differences of I/I_0 values for p(AAPBA-*b*-AGA) or p(AAPBA-*r*-AGA) nanoparticles were attributed to the different contents of AAPBA moiety in copolymers. With the increasing content of AAPBA moiety, relatively less dissociation in nanoparticles occurred after the treatment with 3 mg/mL of glucose, thus leding to less decrease in I/I_0 values. Furthermore, the difference of I/I_0 values between p(AAPBA-*b*-AGA) and p(AAPBA-*r*-AGA) nanoparticles with the similar composition may have originated from different structures of block and random copolymers and different characteristics of self-assembled structures. Compared with block copolymer nanoparticles, there was more association between boronic acid and diols in random ones during the formation process of polymer nanoparticles. Therefore, there

DOI: 10.1021/acs.biomac.5b01020
Biomacromolecules XXXX, XXX, XXX−XXX

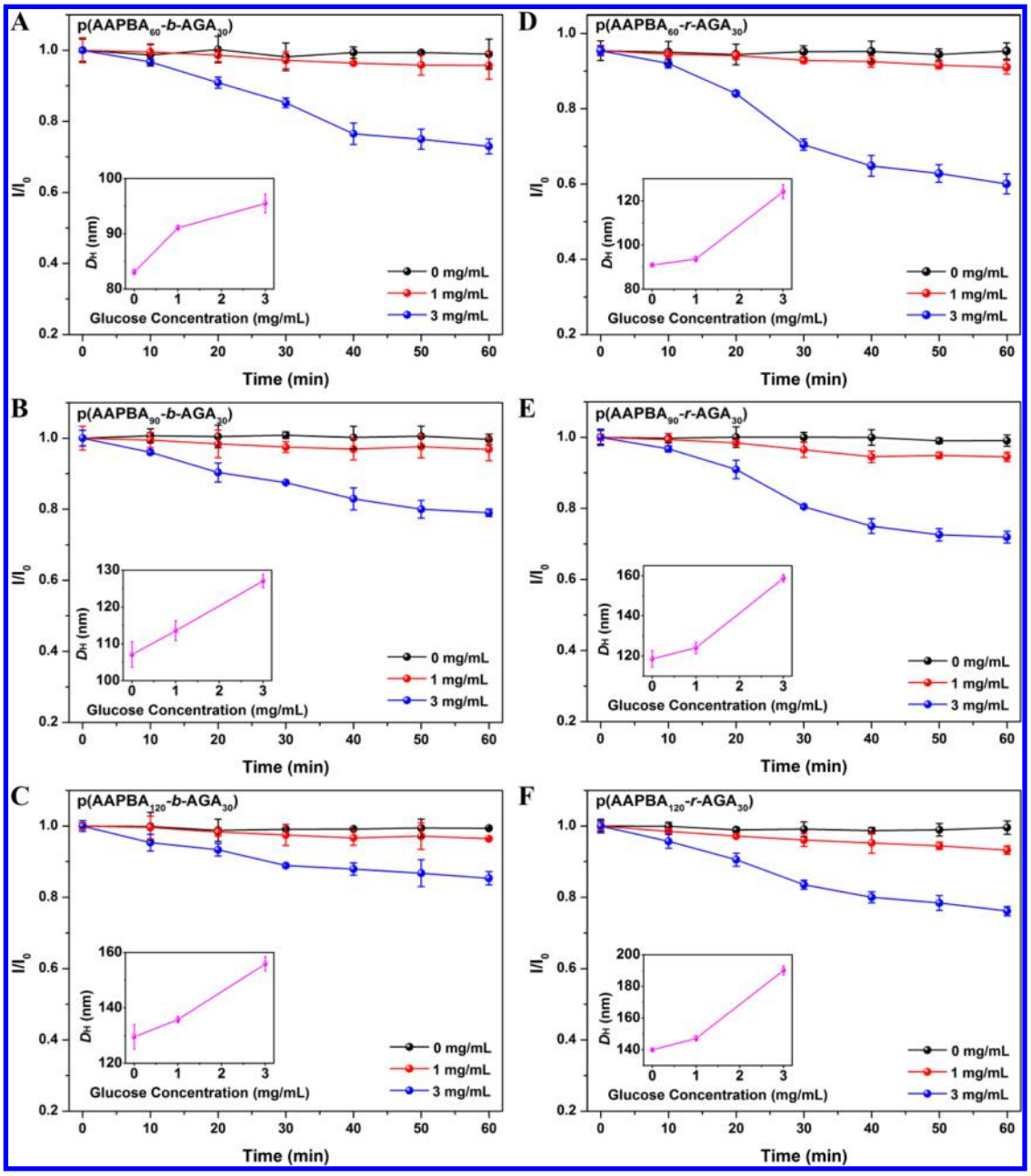

Figure 8. Light scattering intensity of p(AAPBA-*b*-AGA) nanoparticles (A–C) and p(AAPBA-*r*-AGA) (C–E) as a function of time in pH 7.4 PBS. The concentration of both nanoparticles was 1.2 mg/mL. The inset graphs represent size variation responding to 0, 1, and 3 mg/mL glucose concentrations in pH 7.4 PBS.

was more dissociation of nanoparticles in higher glucose medium for random copolymer nanoparticles, resulting in a larger swelling level and greater decrease in I/I_0 values.

Figure 9 showed glucose-sensitive behaviors of block and random copolymer nanoparticles in different glucose media from 0 to 20 mg/mL. Nanoparticles without glucose treatment remained relatively stable during the determined time span. It was found that the light scattering intensity of nanoparticles with higher concentration gradually reduced and subsequently leveled off with increasing glucose concentration over 24 h; that is, aggregate dissociation was highly dependent on the concentration of glucose, with higher concentrations leading to faster and more efficient dissociation. As shown in Figure 9, glucose-responsiveness of both nanoparticles with a lower concentration displayed that aggregate dissociation was rapid and efficient for all glucose media. After the addition of glucose, I/I_0 was reduced with the increase of glucose concentration due to the swelling and dissociation of nanoparticles triggered by glucose. After 8 h, I/I_0 curves reached a plateau which was ascribed to achieving homeostasis of dissociation and association between phenylboronic acid and glucose in the solution.[33,64,67,68] However, we found an abnormal phenomenon shown in Figure 9, I/I_0 final values at 5 mg/mL of glucose solution were 0.56 and 0.53 for p($AAPBA_{120}$-*b*-AGA_{30}) and p($AAPBA_{120}$-*r*-AGA_{30}), respectively, while I/I_0 final values in higher glucose concentration medium were 0.25–0.30 and 0.20–0.28 for them, respectively. That is, I/I_0 curves decreased less than that under other higher glucose concentration although it also reached a plateau after 8 h, indicating that the lower glucose concentration was insufficient to dissociate

DOI: 10.1021/acs.biomac.5b01020
Biomacromolecules XXXX, XXX, XXX–XXX

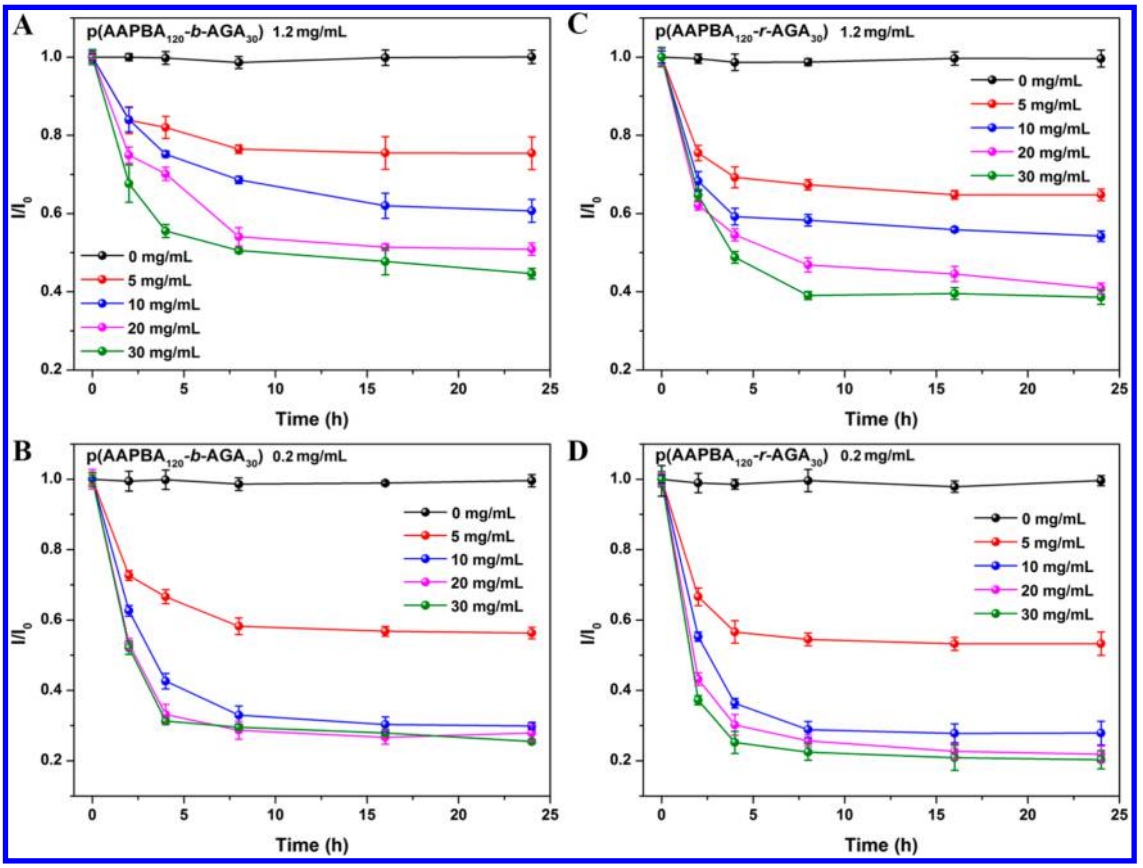

Figure 9. Light scattering intensity of block and random copolymer nanoparticles in different glucose media as a function of time in pH 7.4 PBS. p(AAPBA$_{120}$-*b*-AGA$_{30}$) (A and B); p(AAPBA$_{120}$-*r*-AGA$_{30}$) (C and D).

compact nanoparticles. According to Figures 8 and 9, we can draw a conclusion that random polymer nanoparticles have higher responsive rate and better sensitive ability than block glycopolymer nanoparticles.

Insulin Encapsulation and in Vitro Release. Insulin, a protein containing hydrophilic and hydrophobic amino acid residues, can form stable complexes with polymers.[43,44,69] Moreover, previous works show that amphiphilic phenylboronic acid-based glycopolymer and insulin could self-assemble to fabricate special structure by some interactions such as hydrophobic−hydrophilic interaction, electrostatic interaction, hydrogen bonding and other intermolecular interactions.[11,12,33−38,43,44] Figure 6 showed the size of insulin-loaded nanoparticles. After insulin was encapsulated into nanoparticles, size of p(AAPBA-*b*-AGA) and p(AAPBA-*r*-AGA) nanoparticles was in the range of 123−220 and 119−214 nm, respectively, with narrow size distribution, indicating that insulin was successfully encapsulated into nanoparticles. Moreover, LC of insulin was up to 12.9% for p(AAPBA$_{120}$-*b*-AGA$_{30}$), while that was 10.4% for p(AAPBA$_{120}$-*r*-AGA$_{30}$) (Table 2). The possible reason why block copolymer nanoparticles had higher efficiency was the more compact core−shell structure than the random copolymer nanoparticles.

To explore the potential using the nanoparticles as vehicles in diabetes treatment, the insulin released behaviors from drug-loaded nanoparticles in response to different glucose media (0, 1, and 3 mg/mL) were evaluated. As shown in Figure 10, the release profiles p(AAPBA$_{120}$-*b*-AGA$_{30}$) and p(AAPBA$_{120}$-*r*-AGA$_{30}$) indicated a burst release phase within the first 2 h, which was caused by some insulin that was adsorbed onto the surface during preparation process of nanoparticles. When changing the glucose media from 0 to 3 mg/mL, the burst of insulin increased from 8% to 12% for p(AAPBA$_{120}$-*b*-AGA$_{30}$), and from 10% to 24% for p(AAPBA$_{120}$-*r*-AGA$_{30}$). Meanwhile, the amounts of insulin released after 48 h, in the same release medium, increased from 19% to 58% for p(AAPBA$_{120}$-*b*-AGA$_{30}$), and from 21% to 66% for p(AAPBA$_{120}$-*r*-AGA$_{30}$). Obviously, insulin release from both nanoparticles displayed a biphasic pattern with strong glucose dependence.

Release profiles of insulin from insulin-loaded block and random copolymer nanoparticles upon exposure to 3 mg/mL glucose in pH 7.4 PBS was exhibited in Figure 10. It was found that 7.5%, 10.3%, and 6.5% insulin was released for (AAPBA$_{60}$-*b*-AGA$_{30}$), p(AAPBA$_{90}$-*b*-AGA$_{30}$), and p(AAPBA$_{120}$-*b*-AGA$_{30}$) after 2 h in the first phase comparing with 12.3%, 7.5%, and 6.7% for p(AAPBA$_{60}$-*r*-AGA$_{30}$), p(AAPBA$_{90}$-*r*-AGA$_{30}$), and p(AAPBA$_{120}$-*r*-AGA$_{30}$), respectively. In the second phase, the release rate of insulin gradually decreased and the amount of insulin released after 48 h was 58.0%, 43.8%, and 28.0% for p(AAPBA$_{60}$-*b*-AGA$_{30}$), p(AAPBA$_{90}$-*b*-AGA$_{30}$), and p-(AAPBA$_{120}$-*b*-AGA$_{30}$) and 66.1%, 50.4%, and 37.4% for p(AAPBA$_{60}$-*r*-AGA$_{30}$), p(AAPBA$_{90}$-*r*-AGA$_{30}$), and p-(AAPBA$_{120}$-*r*-AGA$_{30}$), respectively. It is found that the release amount of insulin decreased as content of AAPBA increased in copolymers, which was probably because the polymer hydrophobility enhanced with the increase of AAPBA moieties. By contrast, two kinds of nanoparticles had similar burst release behavior. For the copolymers with the same AAPBA content, the cumulative insulin release of random copolymer nanoparticles was higher than that of block ones. The possible

DOI: 10.1021/acs.biomac.5b01020
Biomacromolecules XXXX, XXX, XXX−XXX

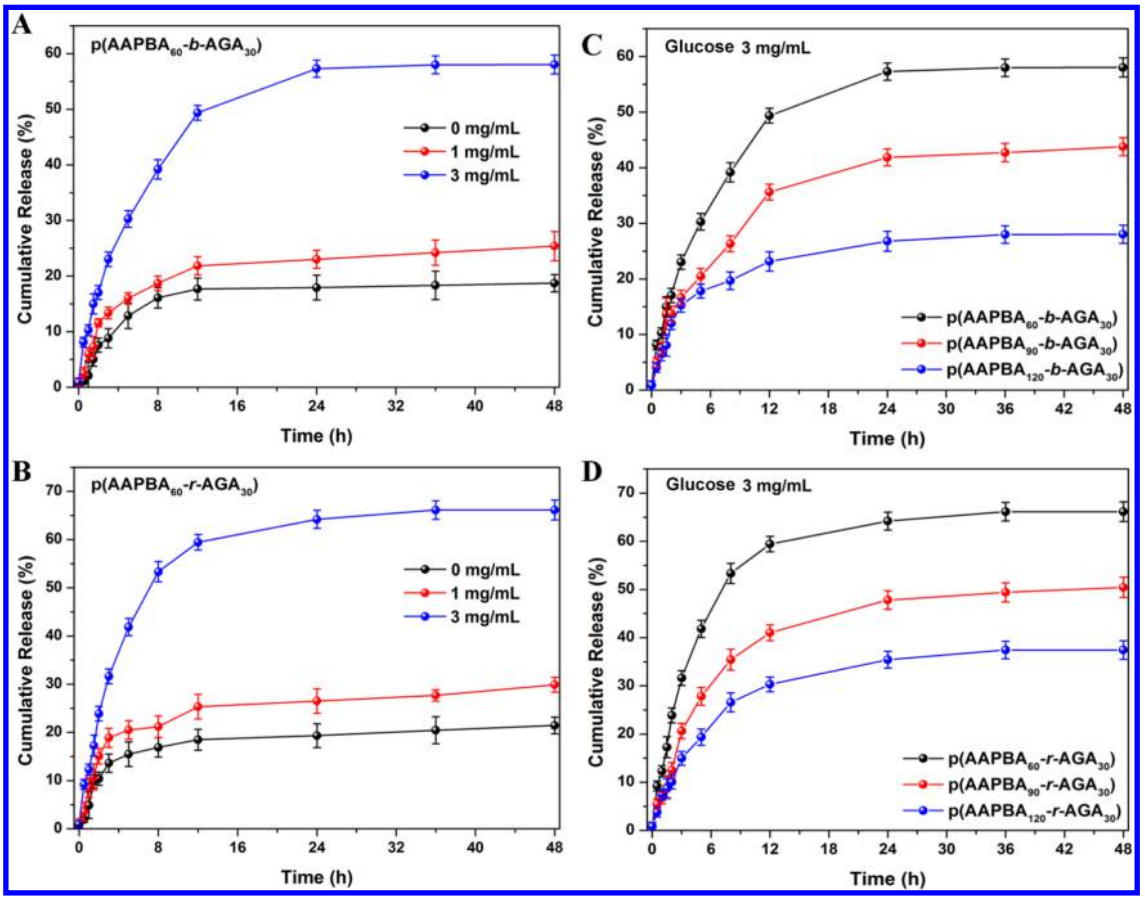

Figure 10. *In vitro* cumulative release of insulin in pH 7.4 PBS from (A) p(AAPBA$_{60}$-*b*-AGA$_{30}$) nanoparticles and (B) p(AAPBA$_{60}$-*r*-AGA$_{30}$) nanoparticles; (C) block copolymer nanoparticles and (D) random copolymer nanoparticles in 3 mg/mL of glucose medium.

Table 4. Drug Release Kinetic Data for the Copolymer Nanoparticles Obtained from Fitting Drug Release Data to the Ritger-Peppas Equation[a]

		Ridger-Peppas model			
samples	glucose concentration (mg/mL)	*n*	*k*	R^2	transport mechanism
p(AAPBA$_{60}$-*b*-AGA$_{30}$)	3	0.4657	12.44	0.9475	non-Fickian diffusion
p(AAPBA$_{90}$-*b*-AGA$_{30}$)	3	0.4688	9.050	0.9366	non-Fickian diffusion
p(AAPBA$_{120}$-*b*-AGA$_{30}$)	3	0.4497	7.404	0..9157	non-Fickian diffusion
p(AAPBA$_{60}$-*r*-AGA$_{30}$)	3	0.6315	14.07	0.9767	non-Fickian diffusion
p(AAPBA$_{90}$-*r*-AGA$_{30}$)	3	0.5339	8.766	0.9153	non-Fickian diffusion
p(AAPBA$_{120}$-*r*-AGA$_{30}$)	3	0.4973	7.300	0.9317	non-Fickian diffusion

[a] *n*, diffusion exponent; *k*, kinetic constant; R^2, correlation coefficient.

reason for the phenomenon was that block copolymer nanoparticles have more compact structure comparing with random ones, leading to lower release of insulin even if in 3 mg/mL glucose medium.

To elucidate the release mechanism, release results were analyzed using the Ritger-Peppas equations. The results in Table 4 show that R^2 values were higher than 0.9, and the values of *n* were in the range 0.45−0.63, indicating that insulin release was mainly non-Fickian diffusion.

Cell Viability. Since the boronated moieties and their derivatives have cytotoxic activity in multiple cell lines, it is necessary to verify the innocuous nature of the polymerized carhydrate moieties present in these copolymers. In this study, in vitro cytotoxicity of p(AAPBA-*b*-AGA) and p(AAPBA-*r*-AGA) on NIH3T3 cells was carried out and analyzed by MTT method. As shown in Figure 11, the cells were exposed to various concentrations of the glycopolymer nanoparticles solutions and incubated for 24 h. For all of the culture, the relative cell proliferation rates were more than 80%, irrespective of copolymer nanoparticle concentration, indicating that the presence of the copolymer did not negatively impact cell proliferation. Moreover, the relative cell proliferation rates increased as the content of carbohydrate moieties in the copolymer increased. All together, carbohydrate moieties enhance the biocompatibility of the phenylboronic acid-based copolymers, and these copolymers have a potential application for in vivo insulin delivery.

DOI: 10.1021/acs.biomac.5b01020
Biomacromolecules XXXX, XXX, XXX−XXX

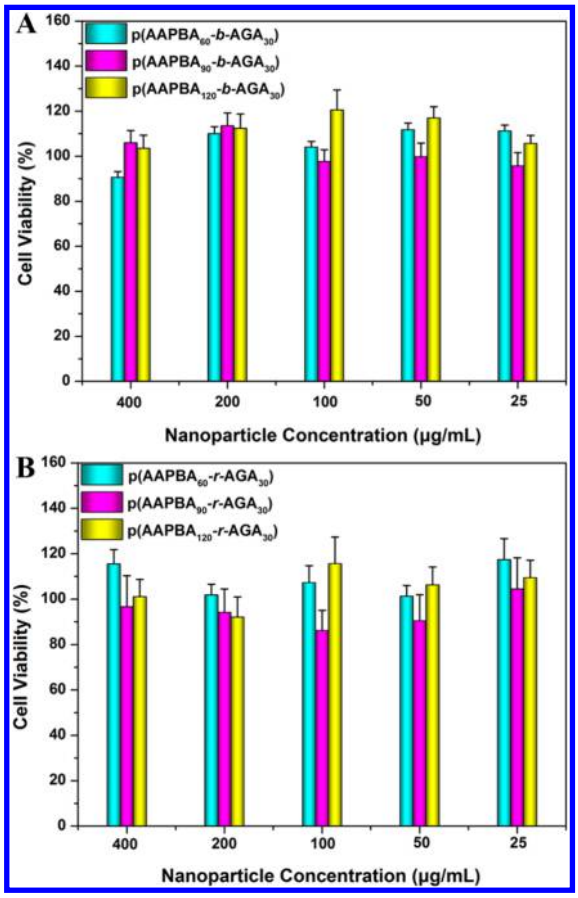

Figure 11. Cell viability of (A) p(AAPBA-*b*-AGA) and (B) p(AAPBA-*r*-AGA) as a function of nanoparticle concentrations by MTT assay at 37 °C after incubation for 24 h. Each value represented the mean ± SD (n = 5).

CONCLUSIONS

In the current study, we synthesized the amphiphilic block and random copolymers based on phenylboronic acid by RAFT polymerization. The two copolymers presented different thermostability due to the different copolymer structures. Both copolymers could self-assemble into stable spherical nanoparticles with narrow size distribution and size of both nanoparticles increased with the increasing glucose concentration. By comparing the glucose-sensitive behaviors, it was found that block copolymer nanoparticles had a more regular T % change than random ones in different glucose media, while there was a more evident variation of size and quicker decreasing tendency in I/I_0 variation action in different glucose concentration media for the random ones. As a glucose-sensitive matrix, insulin was encapsulated into the copolymer nanoparticles, and the release presented glucose dependence pattern. For random copolymer nanoparticles, insulin had a quicker release rate and more cumulative amounts than those from the block ones. The biocompatibility of phenylboronic acid was improved by introduction of carbohydrate moieties, ensuring copolymers with potential application in biomedical fields. In conclusion, the data indicate that the amphiphilic copolymer structure plays an important role in self-assembled nanoaggregates and their glucose-sensitive behaviors.

ASSOCIATED CONTENT

Supporting Information

The Supporting Information is available free of charge on the ACS Publications website at DOI: 10.1021/acs.biomac.5b01020.

^{1}H NMR spectra (Figures S1 and S2) of two monomers and polymers (PDF)

AUTHOR INFORMATION

Corresponding Author

*Address: Key Laboratory of Functional Polymer Materials of Ministry Education, Institute of Polymer Chemistry, Nankai University, Tianjin 300071, China. Tel: +86-22-23501645. Fax: +86-22-23505598. E-mail: zhangxinge@nankai.edu.cn.

Notes

The authors declare no competing financial interest.

ACKNOWLEDGMENTS

This work was supported by the National Natural Science Foundation of China (No. 51173085 and 21474055), the Natural Science Foundation of Tianjin, China (Grant No. 14JYBJC29400), Specialized Research Fund for the Doctoral Program of Higher Education (20130031110014) and Program for Changjiang Scholars and Innovative Research Team in University of Ministry of Education of China (IRT1257).

REFERENCES

(1) Shuai, X. T.; Ai, H.; Nasongkla, N.; Kim, S.; Gao, J. *J. Controlled Release* **2004**, *98*, 415−426.
(2) Meng, Q. Y.; Tian, L. M.; Wang, J. X. *J. Mater. Sci.: Mater. Med.* **2012**, *23*, 991−998.
(3) Sagnella, S. M.; Duong, H.; MacMillan, A.; Boyer, C.; Whan, R.; McCarroll, J. A.; Davis, T. P.; Kavallaris, M. *Biomacromolecules* **2014**, *15*, 262−275.
(4) Yhaya, F.; Lim, J.; Kim, Y.; Liang, M.; Gregory, A. M.; Tenzel, M. H. *Macromolecules* **2011**, *44*, 8433−8445.
(5) Yin, L. G.; Dalsin, M. C.; Sizovs, A.; Reineke, T. M.; Hillmyer, M. A. *Macromolecules* **2012**, *45*, 4322−4332.
(6) Lee, E. S.; Na, K.; Bae, Y. H. *J. Controlled Release* **2005**, *103*, 405−418.
(7) Wei, H.; Zhang, X. Z.; Zhou, Y.; Cheng, S. X.; Zhuo, R. X. *Biomaterials* **2006**, *27*, 2028−2034.
(8) Suzuki, A.; Tanaka, T. *Nature* **1990**, *346*, 345−347.
(9) Horkay, F.; Tasaki, I.; Basser, P. J. *Biomacromolecules* **2000**, *1*, 84−90.
(10) Wang, G.; Tian, W. J.; Huang, J. P. *J. Phys. Chem. B* **2006**, *110*, 10738−10745.
(11) Gu, Z.; Dang, T. T.; Ma, M. L.; Tang, B. C.; Cheng, H.; Jiang, S.; Dong, Y. Z.; Zhang, Y. L.; Anderson, D. G. *ACS Nano* **2013**, *7*, 6758−6766.
(12) Gu, Z.; Aimetti, A. A.; Wang, Q.; Dang, T. T.; Zhang, Y. L.; Veiseh, O.; Cheng, H.; Langer, R. S.; Anderson, D. G. *ACS Nano* **2013**, *7*, 4194−4201.
(13) Kim, H.; Kang, Y. J.; Kang, S.; Kim, K. T. *J. Am. Chem. Soc.* **2012**, *134*, 4030−4033.
(14) Wu, W. T.; Mitra, N.; Yan, E. C. Y.; Zhou, S. Q. *ACS Nano* **2010**, *4*, 4831−4839.
(15) International Diabetes Federation, 2011, http://www.idf.org/media-events/press-releases/2011.
(16) Owens, D. R.; Zinman, B.; Bolli, G. B. *Lancet* **2001**, *358*, 739−746.
(17) Schiel, R.; Müller, U. A. *Exp. Clin. Endocrinol. Diabetes* **2007**, *115*, 627−633.
(18) Kazda, C.; Hülstrunk, H.; Helsberg, K.; Langer, F.; Forst, T.; Hanefeld, M. *J. Diabetes Complications* **2006**, *20*, 145−152.

DOI: 10.1021/acs.biomac.5b01020
Biomacromolecules XXXX, XXX, XXX−XXX

(19) Hemkens, L. G.; Grouven, U.; Bender, R.; Günster, C.; Gutschmidt, S.; Selke, G. W.; Sawicki, P. T. *Diabetologia* **2009**, *52*, 1732−1744.
(20) Rosenstock, J.; Fonseca, V.; McGill, J. B.; Riddle, M.; Hallé, J. P.; Hramiak, I.; Johnston, P.; Davis, M. *Diabetologia* **2009**, *52*, 1971−1973.
(21) Lapeyre, V.; Gosse, I.; Chevreux, S.; Ravaine, V. *Biomacromolecules* **2006**, *7*, 3356−3363.
(22) Ryu, J.-H.; Jiwpanich, S.; Chacko, R.; Bickerton, S.; Thayumanavan, S. *J. Am. Chem. Soc.* **2010**, *132*, 8246−8247.
(23) Ryu, J. H.; Chacko, R. T.; Jiwpanich, S.; Bickerton, S.; Babu, R. P.; Thayumanavan, S. *J. Am. Chem. Soc.* **2010**, *132*, 17227−17235.
(24) Jiwpanich, S.; Ryu, J.-H.; Bickerton, S.; Thayumanavan, S. *J. Am. Chem. Soc.* **2010**, *132*, 10683−10685.
(25) Norris, D. A.; Puri, N.; Sinko, P. J. *Adv. Drug Delivery Rev.* **1998**, *34*, 135−154.
(26) Jung, T.; Kamm, W.; Breitenbach, A.; Kaiserling, E.; Xiao, J. X.; Kissel, T. *Eur. J. Pharm. Biopharm.* **2000**, *50*, 147−160.
(27) Lin, Y. H.; Mi, F. L.; Chen, C. T.; Chang, W. C.; Peng, S. F.; Liang, H. F.; Sung, H. W. *Biomacromolecules* **2007**, *8*, 146−152.
(28) Lin, Y. H.; Chang, C. H.; Wu, Y. S.; Hsu, Y. M.; Chiou, S. F.; Chen, Y. J. *Biomaterials* **2009**, *30*, 3332−3342.
(29) Srinivas, G.; Devalapally, H.; Shahiwala, A.; Amiji, M. *J. Controlled Release* **2008**, *126*, 187−204.
(30) Aboubakar, M.; Couvreur, P.; Pinto-Alphandary, H.; Gouritin, B.; Lacour, B.; Farinotti, R.; Puisieux, F.; Vauthier, C.; et al. *Drug Dev. Res.* **2000**, *49*, 109−117.
(31) Jin, Q.; Lv, L. P.; Liu, G. Y.; Xu, J. P.; Ji, J. *Polymer* **2010**, *51*, 3068−3074.
(32) Kitano, S.; Hisamitsu, I.; Koyama, Y.; Kataoka, K.; Okano, T.; Sakurai, Y. *Polym. Adv. Technol.* **1991**, *2*, 261−264.
(33) Ma, R. J.; Yang, H.; Li, Z.; Liu, G.; Sun, X. C.; Liu, X. J.; An, Y. L.; Shi, L. Q. *Biomacromolecules* **2012**, *13*, 3409−3417.
(34) Cambre, J. N.; Roy, D.; Sumerlin, B. S. *J. Polym. Sci., Part A: Polym. Chem.* **2012**, *50*, 3373−3382.
(35) Kataoka, K.; Miyazaki, H. *Macromolecules* **1994**, *27*, 1061−1062.
(36) Guo, Q. Q.; Wu, Z. M.; Zhang, X. G.; Sun, L.; Li, C. X. *Soft Matter* **2014**, *10*, 911−920.
(37) Cheng, C.; Zhang, X. G.; Wang, Y. X.; Sun, L.; Li, C. X. *New J. Chem.* **2012**, *36*, 1413−1421.
(38) Wang, Y. X.; Zhang, X. G.; Han, Y. C.; Cheng, C.; Li, C. X. *Carbohydr. Polym.* **2012**, *89*, 124−131.
(39) Wang, B. L.; Ma, R. J.; Liu, G.; Liu, X. J.; Gao, Y. H.; Shen, J. Y.; An, Y. L.; Shi, L. Q. *Macromol. Rapid Commun.* **2010**, *31*, 1628−1634.
(40) Tian, F.; Yu, Y. Y.; Wang, C. C.; Yang, S. *Macromolecules* **2008**, *41*, 3385−3388.
(41) Chi, X. D.; Ji, X. F.; Xia, D. Y.; Huang, F. H. *J. Am. Chem. Soc.* **2015**, *137*, 1440−1443.
(42) Meng, Q. Y.; Tian, L. M.; Wang, J. X. *J. Mater. Sci.: Mater. Med.* **2012**, *23*, 991−998.
(43) Zheng, C.; Guo, Q. Q.; Wu, Z. M.; Sun, L.; Zhang, Z. P.; Li, C. X.; Zhang, X. G. *Eur. J. Pharm. Sci.* **2013**, *49*, 474−482.
(44) Jin, X. J.; Zhang, X. G.; Wu, Z. M.; Teng, D. Y.; Zhang, X. J.; Wang, Y. X.; Wang, Z.; Li, C. X. *Biomacromolecules* **2009**, *10*, 1337−1345.
(45) Niemiec, A.; Loh, W. *J. Phys. Chem. B* **2008**, *112*, 727−733.
(46) Barz, M.; Luxenhofer, R.; Zentel, R.; Kabanov, A. V. *Biomaterials* **2009**, *30*, 5682−5690.
(47) Wang, Y. Q.; Xu, J. J.; Zhang, Y. H.; Yan, H. S.; Liu, K. L. *Macromol. Biosci.* **2011**, *11*, 1499−1504.
(48) Oda, Y.; Kanaoka, S.; Sato, Y.; Aoshima, S.; Kuroda, K. *Biomacromolecules* **2011**, *10*, 3581−3591.
(49) Shao, Y.; Jia, Y. G.; Shi, C.; Luo, J.; Zhu, X. X. *Biomacromolecules* **2014**, *15*, 1837−1844.
(50) Xiang, T.; Zhang, L. S.; Wang, R.; Xia, Y.; Su, B. H.; Zhao, C. S. *J. Colloid Interface Sci.* **2014**, *432*, 47−56.
(51) Ferguson, C. J.; Hughes, R. J.; Nguyen, D. *Macromolecules* **2005**, *38*, 2191−2204.
(52) Aqil, A.; Qiu, H.; Greisch, J. F. *Polymer* **2008**, *49*, 1145−1153.
(53) Ting, S. R. S.; Min, E. H.; Zetterlund, P. B.; Stenzel, M. H. *Macromolecules* **2010**, *43*, 5211−5221.
(54) Lee, M. C.; Kabilan, S.; Hussain, A.; Yang, X. P.; Blyth, J.; Lowe, C. R. *Anal. Chem.* **2004**, *76*, 5748−5755.
(55) Roy, D.; Cambre, J. N.; Sumerlin, B. S. *Chem. Commun.* **2008**, *21*, 2477−2479.
(56) Peroche, S.; Degobert, G.; Putaux, J. L.; Blanchin, M. G.; Fessi, H.; Parrot-Lopez, H. *Eur. J. Pharm. Biopharm.* **2005**, *60*, 123−131.
(57) Bradford, M. M. *Anal. Biochem.* **1976**, *72*, 248−254.
(58) Peppas, N. K.; Korsmeyer, R. W. CRC Press: Boca Raton, FL, 1987; p109.
(59) Ivanov, A. E.; Galaev, I.; Mattiasson, Y. B. *Macromol. Biosci.* **2005**, *5*, 795−800.
(60) Matsumoto, A.; Yamamoto, K.; Yoshida, R.; Kataoka, K.; Aoyagi, T.; Miyahara, Y. *Chem. Commun.* **2010**, *46*, 2203−2205.
(61) Ferrier, R. J. *Adv. Carbohydr. Chem. Biochem.* **1978**, *35*, 31−80.
(62) Otsuka, H.; Uchimura, E.; Koshino, H.; Okano, T.; Kataoka, K. *J. Am. Chem. Soc.* **2003**, *125*, 3493−3502.
(63) Hoare, T.; Pelton, R. *Macromolecules* **2007**, *40*, 670−678.
(64) Wang, B. L.; Ma, R. J.; Liu, G.; Li, Y.; Liu, X. J.; An, Y. L.; Shi, L. Q. *Langmuir* **2009**, *25*, 12522−12528.
(65) Wu, Z. M.; Zhang, X. G.; Guo, H. L.; Li, C. X.; Yu, D. M. *J. Mater. Chem.* **2012**, *22*, 22788−22796.
(66) Bapat, A. P.; Roy, D.; Ray, J. G.; Savin, D. A.; Sumerlin, B. S. *J. Am. Chem. Soc.* **2011**, *133*, 19832−19838.
(67) Boduroglu, S.; Khoury, J. M. E.; Reddy, D. V.; Rinaldi, P. L.; Hu, J. *Bioorg. Med. Chem. Lett.* **2005**, *15*, 3974−3977.
(68) Li, S. Q.; Davis, E. N.; Anderson, J.; Lin, Q.; Wang, Q. *Biomacromolecules* **2009**, *10*, 113−118.
(69) Yao, Y.; Zhao, L. Y.; Yang, J. J.; Yang, J. *Biomacromolecules* **2012**, *13*, 1837−1844.

DOI: 10.1021/acs.biomac.5b01020
Biomacromolecules XXXX, XXX, XXX−XXX